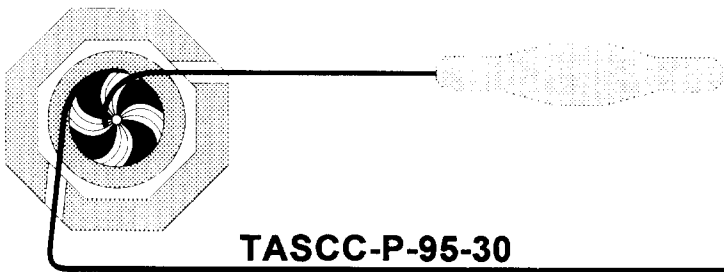


EE



TASCC-P-95-30

PREPRINT

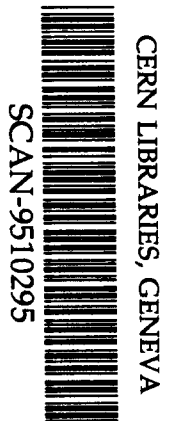
***tascc***

**THE ORIGIN OF SAMPLE MEMORY IN THE  
CHALK RIVER AMS SPUTTER ION SOURCE**

**V.T. Koslowsky, H.R. Andrews, W.G. Davies,  
J.S. Forster and Y. Imahori**

AECL, Chalk River Laboratories, Chalk River, Ontario K0J 1J0, Canada

To be published in the Conference  
Proceedings of ICIS'95,  
6th International Conference on Ion Source,  
Whistler, BC Canada  
1995 September 10-16



SW 9545

**NOTICE**

This report is not a formal publication; if it is cited as a reference, the citation should indicate that the report is unpublished. To request copies our E-Mail address is [TASCC@CRL.AECL.CA](mailto:TASCC@CRL.AECL.CA).

Physical and Environmental Sciences  
Chalk River Laboratories  
Chalk River, ON K0J 1J0 Canada

1995 September

***THE ORIGIN OF SAMPLE MEMORY IN THE  
CHALK RIVER AMS SPUTTER ION SOURCE***

V.T. Koslowsky, H.R. Andrews, W.G. Davies,  
J.S. Forster and Y. Imahori

AECL, Chalk River Laboratories,  
Chalk River, Ontario, Canada K0J 1J0

**Abstract**

The origin of memory effects in the Chalk River AMS sputter ion source has been studied by tracer and elastic-recoil-detection surface analysis techniques. For  $^{36}\text{Cl}$  measurements, the results indicate that the memory arises from contamination of the region immediately surrounding the sample and that it can be mitigated by operating this portion of the ion source above  $350^\circ\text{C}$ . This has reduced memory effects by a factor of 10 or more and has resulted in a similar improvement in background.

## INTRODUCTION

The caesium-sputter ion source has been the source of choice for accelerator mass spectrometry (AMS) because of its efficiency (0.5-10% for C) in producing the negative-ion beams required by the tandem accelerators that are used for AMS work<sup>1)</sup>. In addition these ion sources are relatively simple to construct and operate, and they reliably produce copious ion beams of many elements from small (<1 mg) solid samples. The Chalk River AMS ion source, shown in Figure 1, is typical of many presently in use.

Recent AMS studies<sup>2)</sup> at Chalk River have concentrated on  $^{36}\text{Cl}/\text{Cl}$  and  $^{129}\text{I}/\text{I}$  ratio determinations in many types of samples, including ground water, precipitation, surface waters, soil, air, vegetation, seeds, uranium ore, nuclear fuel and reactor components. The isotopic ratios observed in these samples have varied by several orders of magnitude from  $10^{-8}$  to  $10^{-15}$  depending on the sample and degree of dilution introduced during preparation. Since less than 5% of the sputtered material is extracted as a beam, the remaining material is distributed throughout the ion source and contributes to the ion beam extracted from subsequent samples. This is known as ion-source memory and its effect is to limit the dynamic range of measurements unless the source is dismantled and cleaned. Figure 2 shows the magnitude and time-dependence of the memory in the Chalk

River ion source for Cl. Described below are recent studies that are directed at understanding and mitigating ion-source memory. The issues addressed are the location and mobility of the sputtered material, its correlation with Cs (an active getter) deposition and the effects of temperatures on surface composition. Subsequent sections describe the use of a radioactive tracer  $\text{Ag}^{82}\text{Br}$  to map the distribution of sputtered material, surface-characterization measurements with the elastic recoil detection (ERD) technique<sup>3</sup>, modifications to the source to reduce memory effects and their outcome, and finally some conclusions.

#### **THE SURFACE DISTRIBUTION OF SPUTTERED MATERIAL**

To determine the distribution of sputtered material representative of either Cl or I,  $\text{Ag}^{82}\text{Br}$  ( $t_{1/2}$  - 1.47 d) was prepared in the Chalk River NRU reactor, diluted with Ag powder and packed into a Cu sample holder. Its  $\beta$  decay rate was initially 90 kBq. The sample was subsequently sputtered for 2 hours during which approximately 7% of the sample was consumed. The ion source was then cooled, dismantled and assayed with a 50 mm<sup>2</sup>, 2000  $\mu\text{m}$  thick silicon surface-barrier detector. The distribution of activity was observed to be quite localized, the bulk of it on the aperture surrounding the sample or in the corner formed by the aperture plate and heat shield (see Fig.1). Small quantities of activity were also observed on the ionizer and slits. This was likely due to implantation of the accelerated

negative ion beam. These results suggest that ion-source memory originates from the material deposited around the aperture and/or from the migration of Cl or I from the contaminated regions to the sample location. Measurements of the aperture-plate temperature indicate that it is about 90° at the outer edge and about 130°C mid-radius.

## **SURFACE CHARACTERIZATION BY ELASTIC RECOIL DETECTION**

The elastic recoil detection (ERD) method involves the use of nuclear detection techniques to identify forward-recoiling surface atoms Rutherford-scattered by a heavy-ion beam. In these measurements a 226 MeV Au<sup>21+</sup> beam from the TASSC facility was used. A typical  $\Delta E$ -E spectrum from an ERD measurement of an ion-source component is shown in Figure 3.

The first measurements, which were intended to determine the feasibility of using the ERD technique for ion-source development, involved the analysis of the surface coatings of four plugs removed from the AMS ion source after several days of use. The plug locations, shown in Figure 1, range from the aperture plate to a region far from the sample. The region closest to the sample showed a strong Cl signal which was nearly absent

in the most remote sample. Other major surface constituents were B, C, O, F, Na, Al and the stainless steel constituents, Fe, Cr, Si, etc. Elements C and O are expected on most surfaces; the B likely originates from boron nitride in the ionizer heater; the F, from the fluoroelastomer O-rings; and the Na, as an impurity in the Cs. The source of Al is unknown.

In a second ERD measurement, Cs was evaporated onto a temperature-controlled substrate in the ERD scattering chamber. At about 150°C, it was found that Cs could be driven off the surface and re-adsorption prevented.

The third ERD experiment studied the surface layers of a temperature-controlled heat-shield in a functioning sputter-ion source (see Figure 4) that contained a AgCl sample mounted in a Cu sample holder. Many elements could be identified (see Figure 3) but only the Cs, Ag, Cu, Cl and F layers were observed to thicken with time while the heat shield was below 100°C. The fluorine contamination began to decrease above 100°C, whereas Cl and Cs were not driven off until about 300°C (see Figure 5). The similarity of the Cs and Cl desorption vs. temperature profiles suggest that Cl is bound at the surface in the form of CsCl, since atomic Cs or Cl would be expected to disappear at 150°C or lower. Similarities in the Cs and Cl counting rate also suggests that equal quantities of each were deposited on the surface as the Rutherford cross-sections are similar.

## **MODIFICATIONS TO SOURCE DESIGN AND EFFECTS**

The ERD and tracer measurements suggest that contamination of the region immediately surrounding the sample is the likely cause of the ion-source memory. The contaminated corner regions are too cool to cause significant migration of CsCl. The ion source was therefore modified so that an aperture insert was thermally insulated from its surroundings and radiatively heated by the ionizer to 380°C. No additional heaters were incorporated. The ion source was subsequently used in  $^{129}\text{I}$  and  $^{36}\text{Cl}$  measurements and deliberately contaminated with a  $5 \times 10^{-10}$   $^{36}\text{Cl}/\text{Cl}$  sample. The memory under these conditions is also shown in Figure 2 and has been reduced between one to two orders of magnitude. Relative contamination can be reduced to  $10^{-4}$  in 10 minutes whereas several hundred minutes were required with a cool aperture. The conclusion that a contaminated aperture contributes to ion-source memory is also supported by other  $^{36}\text{Cl}/\text{Cl}$  measurements intended to check for systematic bias caused by partially filled sample holders. Background runs following the runs with partially-filled holders had less contamination than those following runs with full sample holders, possibly indicating that  $^{36}\text{Cl}$  at the bottom of the cavity was unable to reach the aperture due to the shadowing effect of the cavity walls.

The transient response of iodine memory in the AMS ion source has not yet been measured. Iodine-129 background was reduced when compared to earlier  $^{129}\text{I}$  AMS measurements but not to the same degree as that observed for  $^{36}\text{Cl}$ . Further ERD measurements with AgI may help clarify this situation.

## CONCLUSIONS

A combination of tracer and ERD measurements has resulted in simple and effective ion-source design changes that have significantly reduced  $^{36}\text{Cl}$  memory, improved the dynamic measurement range and lowered the routine  $^{36}\text{Cl}/\text{Cl}$  background to about 5 parts in  $10^{16}$ . These diagnostic techniques may also help improve the sensitivity for other AMS isotopes such as  $^{129}\text{I}$  and  $^{14}\text{C}$  and may have applications in solving Secondary Ion Mass Spectrometry and ion-implantation memory problems.



## REFERENCES

1. M. Suter, Nucl. Instr. and Meth. in Phys. Res., B52 (1990) 211.
2. H.R. Andrews, V.T. Koslowsky, R.J.J. Cornett, W.G. Davies, B.F. Greiner, Y. Imahori, J.W. McKay, G.M. Milton and J.C.D. Milton, Nucl. Instr. and Meth. in Phys. Res. B92 (1994) 74.
3. R. Siegele, J.A. Davies, J.S. Forster and H.R. Andrews, Nucl. Instr. and Meth. in Phys. Res., B90 (1994) 606.

## FIGURE CAPTIONS

- Figure 1 Schematic of the Chalk River AMS ion source. The squares mark locations of plugs that were removed and analyzed by ERD for identification of surface constituents.
- Figure 2 Time dependence of  $^{36}\text{Cl}$  memory in the Chalk River AMS ion source during several runs after a high-level  $^{36}\text{Cl}$  sample was introduced into the source. The ordinate is the measured  $^{36}\text{Cl}/\text{Cl}$  atom ratio of a blank Cl sample normalized to the atom ratio of the contaminating sample. The data identified as Jun. 95 were acquired after the aperture, immediately ahead of the sample, was altered to operate at  $\sim 380^\circ\text{C}$ . The scatter in the Jun 95 data is due to counting statistics.
- Figure 3 A  $\Delta E$ -E (energy loss vs. residual energy) spectrum from an ERD measurement. Atomic number is directly related to energy loss whereas depth is inversely related to total energy. For example, surface layers appear as islands (see Cs, Ag); distributions and thick substrates such as Fe or Si appear as nearly-continuous bands. A large number of elements ranging from C to Cs can be easily identified and their counting intensity recorded against time.
- Figure 4 Schematic of ERD experiment that identified surface layers on a temperature-controlled stainless-steel block that was located adjacent to the ion source. In this experiment, beam was not extracted from the source, but Cs sputtered the

sample while a diagnostic Au beam Rutherford-scattered surface atoms off of the block into a  $\Delta E$ -E detector telescope. The block temperature could be controlled between 60 and 400°C.

**Figure 5** Counting rate of Rutherford-scattered surface atoms vs. time. The counting rate is related to surface concentration and is initially slowly increasing for Ag, Cs, Cl, F and Cu (not shown). Other elements visible in the spectrum shown in Figure 3 were constant in surface concentration. As the substrate temperature was increased with time, Ag and Cu continued to accumulate on the surface whereas F, Cl and Cs were desorbed. The initial deposition rate is about  $10^{13}$  atoms/cm<sup>2</sup>/s.

# AMS ION SOURCE

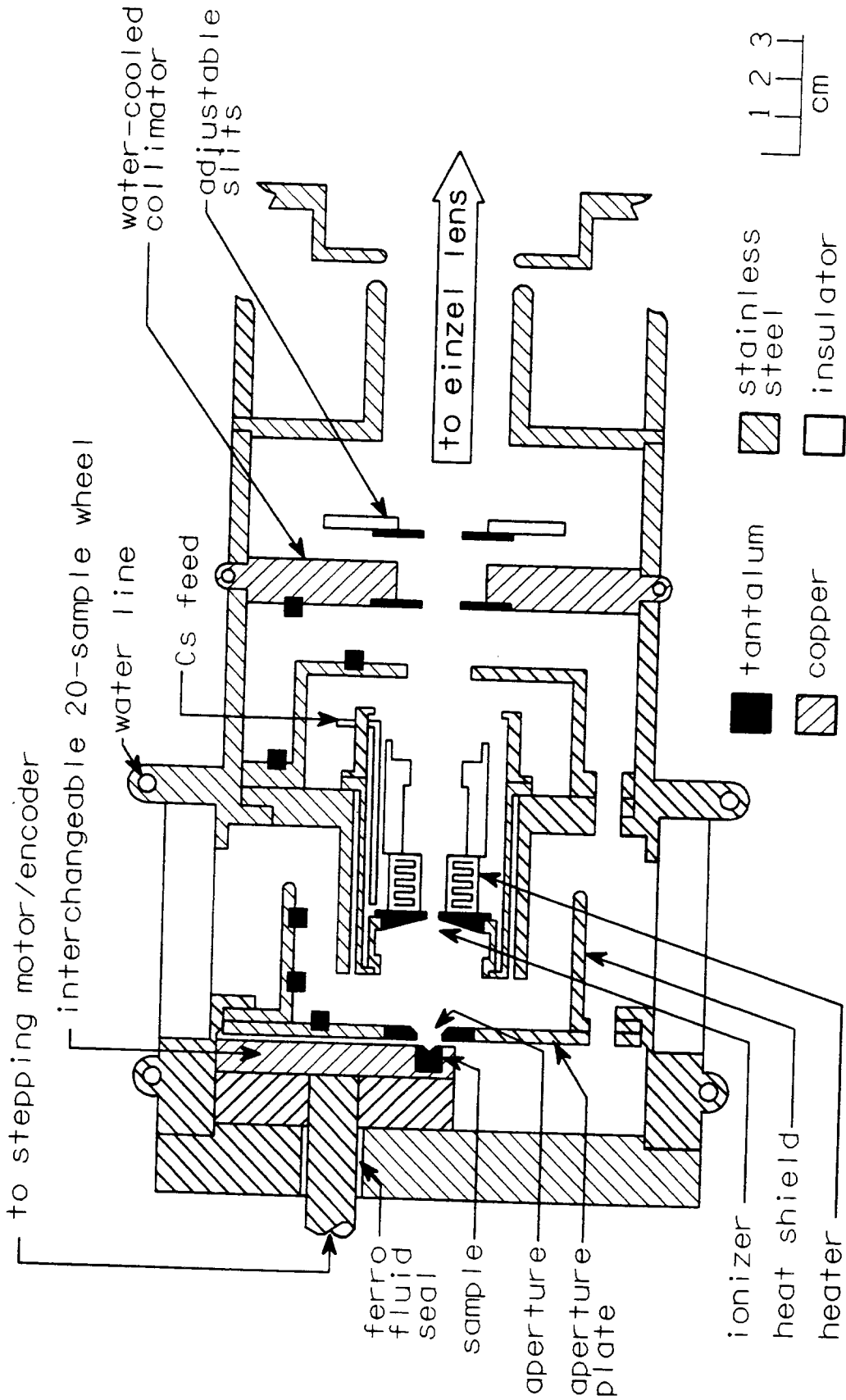


Fig1

# $^{36}\text{Cl}$ Memory

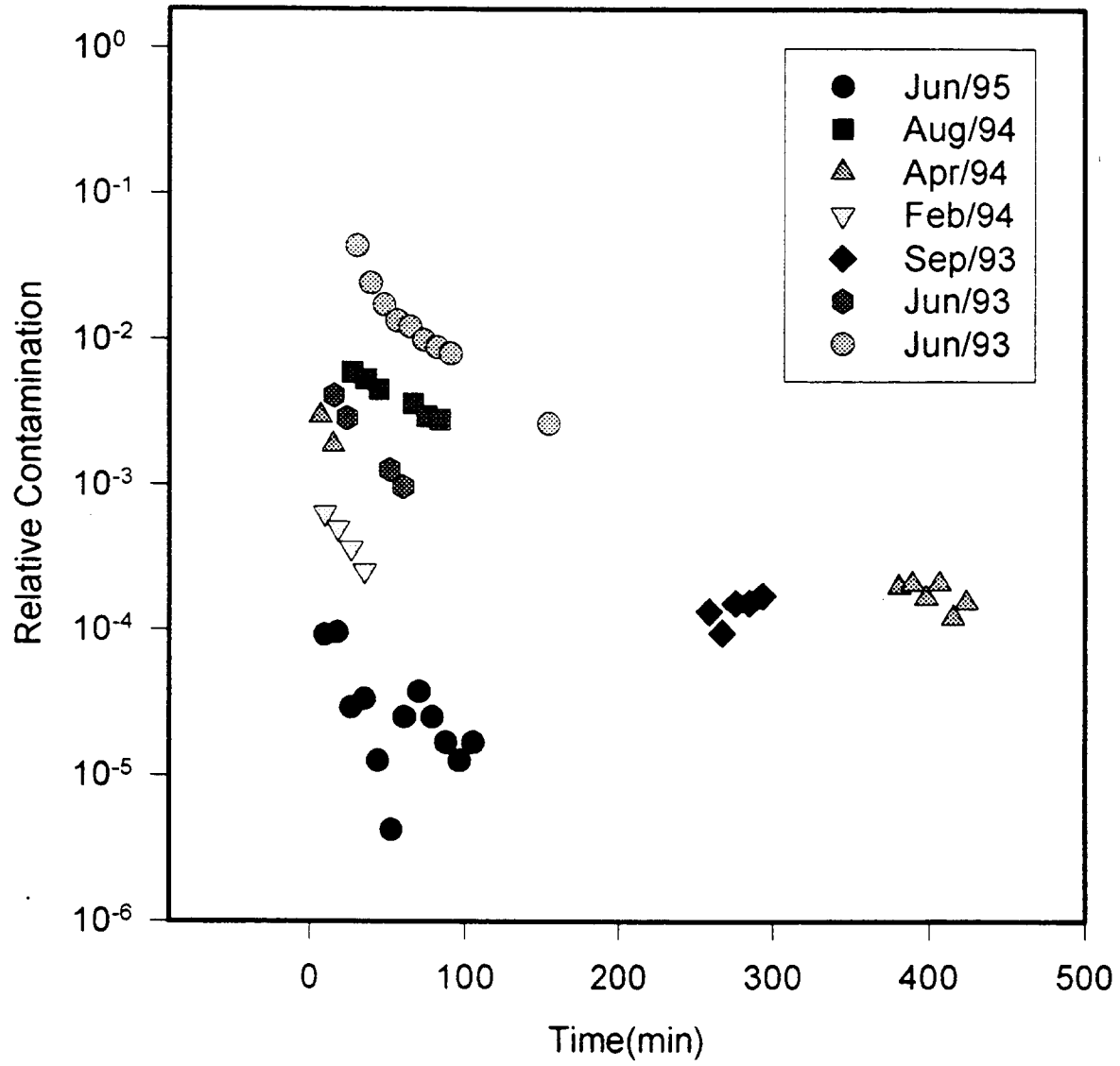


Fig 2

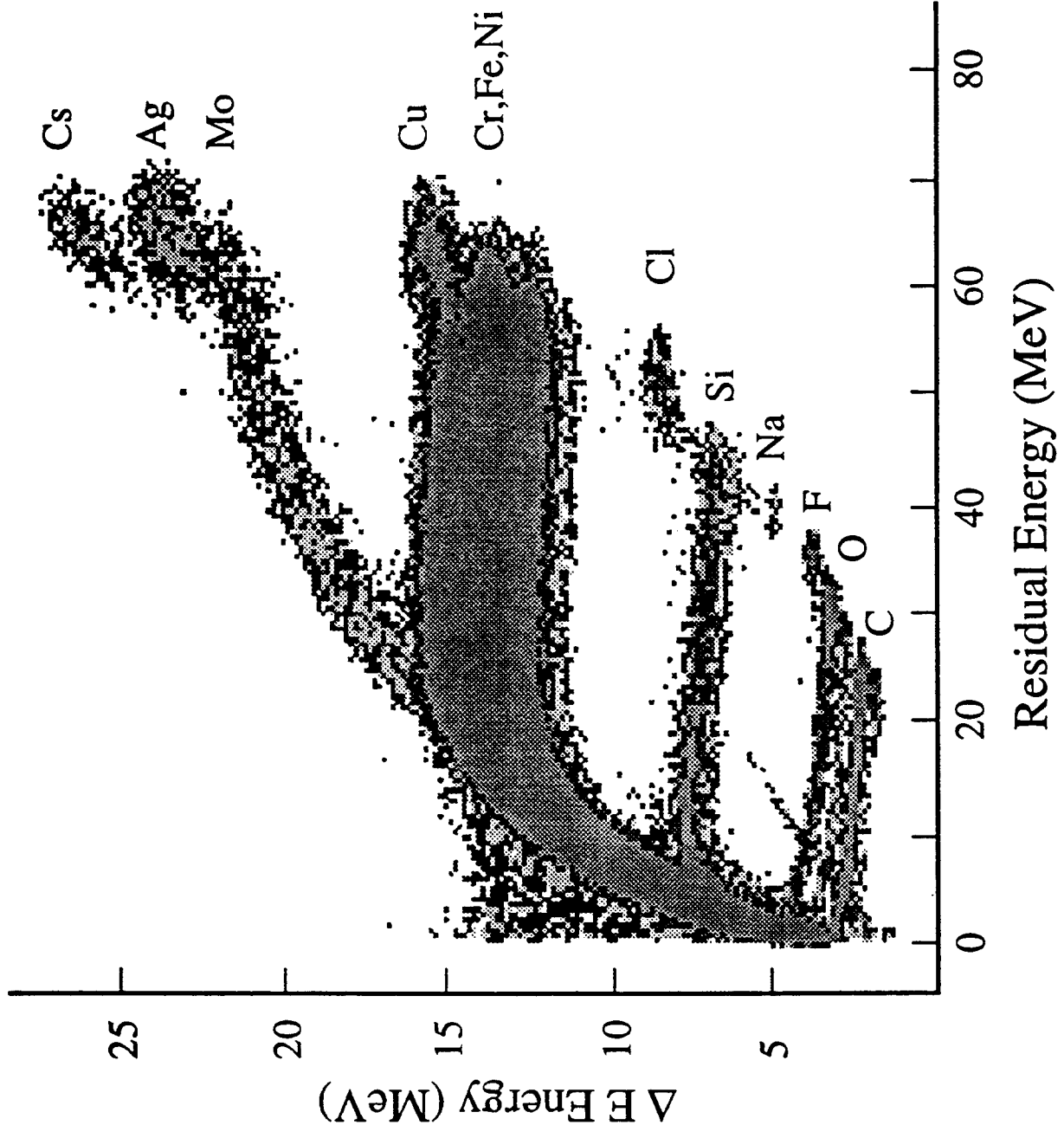


Fig3

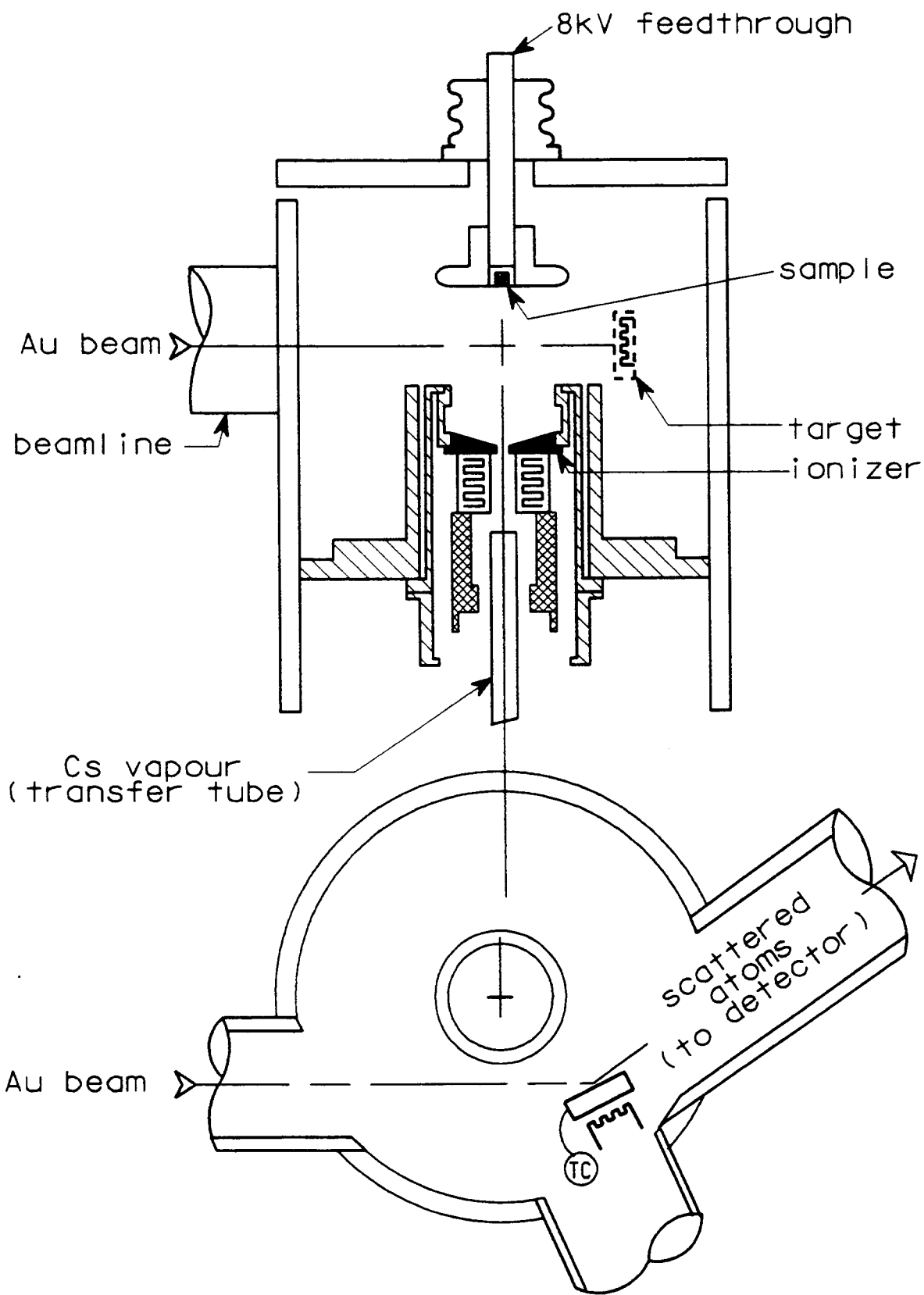


Fig 4

# Thin-Film Thickness .vs. Time

